

## POSSIBLE EFFECTS OF MAGNETIC ACTIVITY IN ORBITAL LIGHT CURVES OF CLOSE BINARIES

JUAN GARCÉS LETELIER<sup>1</sup> , RONALD E. MENNICKENT<sup>1</sup>   
and JELENA PETROVIĆ<sup>2</sup> 

<sup>1</sup>*Universidad de Concepción, Departamento de Astronomía,  
Casilla 160-C, Concepción, Chile  
E-mail: juangarces@udec.cl*

<sup>2</sup>*Astronomical Observatory, Volgina 7, 11060 Belgrade, Serbia*

**Abstract.** In close binary systems with magnetic activity in at least one of their components, distinctive features can be observed in their light curves. This study presents a photometric analysis of several binary systems with at least one active component. We start with a preliminary study of the O'Connell effect in short orbital period binaries identified in the Kepler binary catalog. This phenomenon in the light curves could be attributed to the migration of spots on the surface of the active star, making them key objects for studying the differences between the magnetic fields of isolated stars and those in binary systems. In addition, a comprehensive photometric analysis could reveal unexpected behaviour in the orbital light curves, related to magnetic activity. Recently, we have analysed the light curves of Double Periodic Variables binary systems and found cyclic changes in their orbital light curves, possibly as a consequence of a magnetic dynamo operating in the donor star. These results open up new perspectives for exploring the consequences of stellar magnetism in interacting binaries.

### 1. INTRODUCTION

In close binary systems, a rotation period synchronized with the orbital period and a circularized orbit are expected due to tidal interactions (Zahn 1975, 1977). If one of the components is of F-K spectral type, magnetic activity is enhanced as they transform into rapid rotators compared to single stars (Richards & Albright 1993). Different types of stars show signs of chromospheric or coronal activity, including spotted stars, BY Draconis stars, RS Canum Venaticorum, FK Comae Berenices, solar-type stars, W UMa and Algol-type binary systems, among others (e.g., Pi et al. 2019; Xiang et al. 2020).

One consequence of this magnetic activity is the presence of cold spots on the surface of the active star, some even revealed through Doppler images, as in the case of the prototype binary RS Canum Venaticorum (Xiang et al. 2020). Additionally, these spots generate quasi-periodic variations evidenced in high-precision photometry from space telescopes such as Kepler or TESS (e.g., Tran et al. 2013; Balaji et al. 2015). Some specific effects of these spots in the orbital light curves of binary systems are: i) The O'Connell effect (O'Connell 1951), reflected in the asymmetry of the orbital light curve when comparing maxima near the first and second quadrature. At times, this variation changes over time due to the changing position of the spot on the active stellar surface (e.g., Shi et al. 2021). ii) The anticorrelation in the O-C (observed mi-

nus calculated) diagram, that analyzes the midtimes at which primary and secondary minima occur assuming a constant orbital period (e.g., Tran et al. 2013). Balaji et al. (2015) attributed this phenomenon to changes in the spot position on the active star. Possible explanations for this phenomenon could involve asynchronous rotation of the spotted star, differential rotation at high latitudes of the active star or variable magnetic field configurations (Balaji et al. 2015).

Photometric analysis is crucial in revealing how magnetic activity can affect orbital light curves. In this regard, Double Periodic Variables (DPVs) could play an important role. DPVs are semi-detached binary systems that exhibit two photometric cycles in their light curves: one with an orbital period ( $P_o$ ), typical of eclipsing and ellipsoidal binaries, and another with a long period ( $P_l$ ) characterized by a sinusoidal morphology and an as yet unknown origin (Mennickent et al. 2003). Both periods are closely related, with  $P_l = (31.9 \pm 4.4) \times P_o$  (Rojas García et al. 2021). DPVs are classified as hot Algol systems, where the more evolved A/F/G-type star (donor) has filled its Roche lobe and is transferring mass to a B-type dwarf (gainer) through an optically thick accretion disk (Mennickent 2017).

Spectroscopic studies have demonstrated the presence of high-latitude bipolar wind modulated by the long cycle in the galactic DPV V393 Sco (Mennickent et al. 2012). For the same system, variable chromospheric Mg II, C I, Fe II and Ti II emission lines originating from the secondary star, whose emissivity increases during the maximum phase of the long cycle, has been found (e.g., Mennickent et al. 2012, 2018). It has also been shown that active zones such as the bright/hot spot, produced due to binary interaction, vary depending on the long cycle as a possible consequence of a variable mass transfer rate in HD170582 (Mennickent et al. 2015). These pieces of evidence could be explained in the context of a magnetic dynamo acting on the secondary star. Based on the Applegate (1992) mechanism, Schleicher & Mennickent (2017) suggested that due to magnetic activity, the donor star could change its quadrupolar moment, altering its equatorial radius, and consequently, the mass transfer rate on scales comparable to the long cycle observed in DPVs. This hypothesis could explain structural changes in the accretion disk observed in some DPV systems (e.g., Garcés et al. 2018; Mennickent et al. 2020) due to a mass transfer rate that cyclically varies throughout the long cycle (Mennickent & Djurašević 2021).

Our motivation is the photometric analysis of the light curves of those binary systems where one of its components is magnetically active. In this work, we present a preliminary analysis of binary systems from the Kepler Eclipsing Binary Catalog (Third Revision<sup>1</sup>) (Matijević et al. 2012) that show variations due to the presence of cold spots. Secondly, we will also show some results from the photometric analysis of orbital light curves of DPV binaries, whose morphology changes could be a direct consequence of the magnetic activity of the donor star, opening the door to a little-studied consequence of magnetic activity in orbital light curves.

## 2. METHODS

### 2. 1. KEPLER BINARY SYSTEMS

First, we studied the sample of 412 binary systems from the Kepler catalogue. These binaries were studied by Balaji et al. (2015), who analysed the midtimes at which the

---

<sup>1</sup><http://keplerebs.villanova.edu/>

Table 1: Initial masses considered for the grid of 9x3 models used in the search for the best fit to the luminosity and effective temperature of the OGLE-BLG-ECL-157529 star. The pairs of masses in each column correspond to initial configurations that were evolved considering orbital periods of 4, 5 and 6 days (27 models in total).

Mass [ $M_{\odot}$ ]	Mass [ $M_{\odot}$ ]	Mass [ $M_{\odot}$ ]
3.0-2.5	3.2-2.5	3.4-2.5
3.0-2.7	3.2-2.7	3.4-2.7
3.0-2.9	3.2-2.9	3.4-2.9

primary and secondary minima occur through O-C diagrams, explaining the observed anticorrelated variations with a continuous change in the longitude of a cold spot on the active star.

We used long-cadence photometry from which instrumental effects were removed without affecting the astrophysical variations of each target. We selected the maximum of each orbital cycle using quadratic fitting in the photometry near the maximum of the first ( $Max_I$ ) and second quadrature ( $Max_{II}$ ) to determine the O’Connell effect variation. Subsequently, for each orbital cycle, we derived a value for  $\Delta Mag = Max_I - Max_{II}$ , allowing us to probe how the O’Connell effect varies over time (see Fig. 1). If a periodic variation was detected, we applied the Generalized Lomb-Scargle (GLS) periodogram (Zechmeister & Kurster 2008). Additionally, we performed a smooth mathematical fit to the orbital light curve using Savitzky-Golay filter (Savitzky & Golay 1964). Then, we analyzed the residuals, without the primary and secondary minimum, using the GLS periodogram to search for peaks near the orbital period. We selected these periods and attributed them to the rotational period of the spotted star.

## 2. 2. DPV-TYPE BINARIES

We conducted a photometric analysis based on studies aimed to elucidate the photometric behavior of OGLE-LMC-DPV-097 (Garcés et al. 2018) and OGLE-BLG-ECL-157529 (Mennickent et al. 2020). To achieve this, we performed a light curve disentangling using Fourier series (e.g., Garcés et al. 2018). Then we divided the orbital cycle according to the long cycle phases (see Garcés et al. 2018). As in previous studies, the most drastic changes occur near the secondary minimum of the orbital light curves. Thus, we examined how the depth of the secondary minimum of DPVs from the Poleski et al. (2010) catalogue varies by comparing between the orbital light curve at the maximum and minimum of the long cycle. To do so, we applied a polynomial fit enabling us to estimate the depth of the secondary minimum.

Additionally, we conducted an analysis of the evolutionary state of the OGLE-BLG-ECL-157529 binary system using the stellar evolution code MESA (Paxton et al. 2011, 2013, 2015). We considered a grid of 27 models (see Table 1) and identified the best fit considering observed parameters such as mass, luminosity, and radius of the primary and secondary stars. The best model corresponds to the best fit and thus the lowest  $\chi^2$  value (e.g., Mennickent et al. 2016). Lastly, using the equation 16 from Schleicher & Mennickent (2017), we determined how the ratio between the orbital period and the long period evolves for this system, following the methodology of Mennickent et al. (2018).

Table 2: Theoretical values of luminosity, radius, temperature and masses for the gainer and donor stars of OGLE-BLG-ECL-157529 obtained with MESA compared with those obtained by Mennickent & Djurašević (2021) (M&D) from photometric analysis.

Model	Star	$\log L (L_{\odot})$	R ( $R_{\odot}$ )	$T_{eff}$ (K)	Mass ( $M_{\odot}$ )
MESA	Donor	1.99	16.98	4365	1.17
M&D		$1.96 \pm 0.01$	$16.6 \pm 0.2$	4400 (fixed)	$1.06 \pm 0.2$
MESA	Gainer	2.80	3.16	16218	4.92
M&D		$2.83 \pm 0.10$	$4.48 \pm 0.2$	$14000 \pm 500$	$4.83 \pm 0.3$

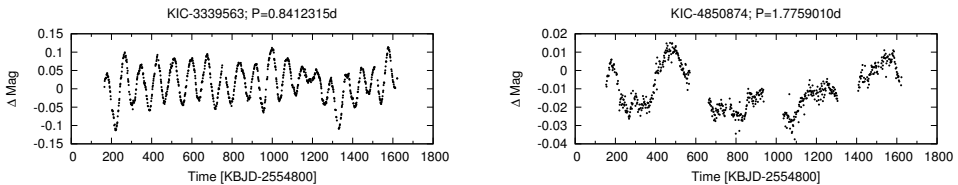


Figure 1: Difference between the observed magnitude of the first and second maxima at the orbital light curve over time (see Sec. 2.1). Left, we showcased an example of cyclic variation in the O’Connell effect, while on the right, we observed non-cyclic variation.

### 3. RESULTS

#### 3.1. KEPLER BINARY SYSTEMS

We noticed that 398 out of the 412 analyzed binaries exhibit a time-variable O’Connell effect. Among them, 163 show periodic or quasi-periodic variations, while 235 binaries display non-periodic variations (see Fig. 1). In addition, we observe that binaries showing cyclic variations in the O’Connell effect have faster rotation periods than the orbital period in most cases. For binaries showing non-periodic variation of the O’Connell effect, we observe that the orbital period and the rotation period are quite similar, with a ratio close to 1. In addition, we observe that the O’Connell effect varies with a cyclicity ranging from approximately 17 to 350 days (see Fig. 2).

#### 3.2. DPV-TYPE BINARIES

We have analyzed 96 DPVs of the Large Magellanic Cloud (LMC). OGLE-LMC-DPV-097 shows the most significant changes and the largest long-cycle amplitude among the DPVs we have considered. Similarly, OGLE-BLG-ECL-157529 shows the most significant changes around the secondary minimum, but its amplitude is similar to other DPVs. We have noticed that 60% DPVs show strong evidence of a deeper secondary minimum at long-cycle maximum, compared to the depth of the secondary minimum at long-cycle minimum. In contrast, only 10% show the opposite case, i.e., a deeper secondary minimum at the long cycle minimum. Finally, 30% show no significant changes, of which 87% have been classified as ellipsoidal (ELL) DPVs, i.e., DPVs with a lower orbital plane inclination than the eclipsing (ECL) ones (see Fig. 3).

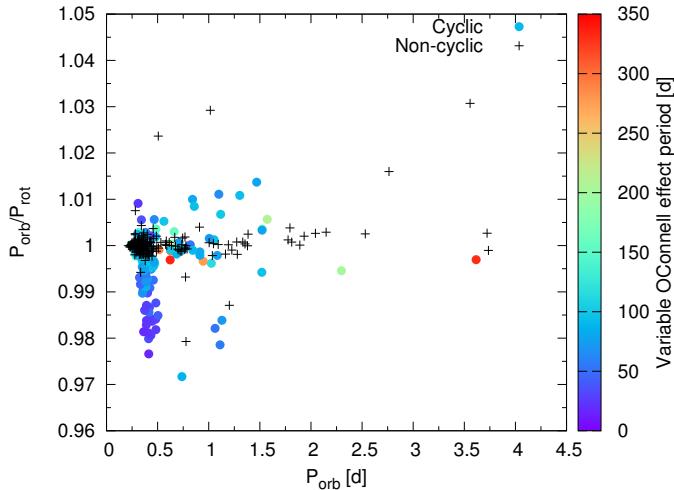


Figure 2: Orbital period versus the ratio of orbital to rotational period for 398 binary systems studied in Balaji et al. (2015). The coloured dots indicate the estimated period in those cases where the variation of the O’Connell effect is cyclic. The black symbols represent those cases where the O’Connell effect varies non-cyclically.

Regarding the evolutionary state, we achieve the best fit to the observed parameters for OGLE-BLG-ECL-157529 by considering a model with initial masses of 3.2 and 2.9  $M_{\odot}$  and an initial orbital period of 6 days. We note that the best fit is attained when the binary system reaches an age of 266.9 Gyr and is undergoing a case-B mass transfer process. Furthermore, by considering equation 16 of Schleicher and Mennickent (2017) and values estimated using MESA for the secondary star’s luminosity, masses, and radius, we have successfully established the evolution of the ratio between the long and orbital periods for this system. Upon comparing this ratio with the observed one, we find a good agreement (see Fig. 4).

#### 4. DISCUSSION

In our preliminary analysis, we have observed a variable O’Connell effect in a significant part of the binaries studied by Balaji et al. (2015). The nature of this phenomenon is not entirely clear, because the origin of the spot migration is not known. As we have seen, for systems where the O’Connell effect varies cyclically, we can estimate the period of a complete rotation of the spot on the surface of the active star. In addition, it is also possible to estimate the lifetime of the spots using autocorrelation functions (Giles et al. 2017, Niu et al 2021). These large-scale analyses could provide information on the behavior of magnetic fields in active stars within binary systems. However, it is essential to first classify the different objects that show magnetic activity and to understand how other binary interaction processes might affect the photometry.

On the other hand, through a photometric analysis of DPV-type binaries, we have demonstrated that 70% of LMC’s DPVs exhibit changes in their orbital light

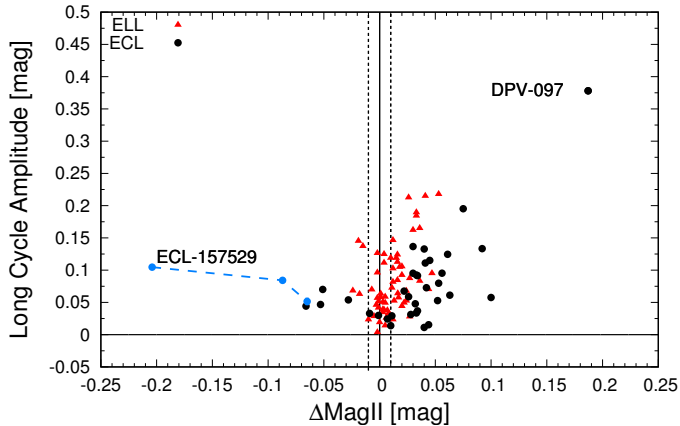


Figure 3:  $\Delta Mag_{II}$  versus long cycle amplitude for the I-band. We note that positive values refer to a secondary minimum deeper during the maximum of the long cycle. In the opposite case, we have negative values. Red points represent the values obtained for the ELLs DPVs and the black ones for the ECLs DPVs. The position of OGLE-LMC-DPV-097 and OGLE-BLG-ECL-157529 is high-lighted because they represent the DPVs with the most drastic changes. Shown in blue is how the long cycle amplitude and depth of the secondary eclipse change according to Mennickent et al. (2020). The dashed vertical lines indicate the range in which no changes in the orbital light curves are observed.

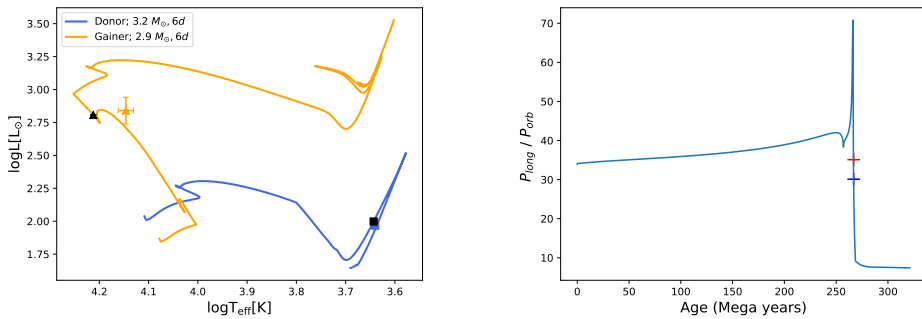


Figure 4: Left: H-R Diagram of OGLE-BLG-ECL-157529. The evolutionary tracks of the primary (in orange) and secondary (in blue) components are presented. The best fit is achieved by considering an initial mass of  $3.2M_{\odot}$  and  $2.9M_{\odot}$  and an initial orbital period of 6 days. The yellow triangle and blue square represent the observed parameters for the primary and secondary components, respectively. The black symbols represent the best fit for the observed parameters (see Table 2). Right: estimation of the variation of the long period to orbital period ratio considering the Schleicher and Mennickent (2017) equations and the values of mass, radius and temperature of the secondary according to the best MESA model for OGLE-BLG-ECL-157529. The red and blue symbols show the observed period ratios (see Mennickent et al. 2020) for the age that best fits the observed data.

curves associated with different phases of the long cycle. Primarily, we've observed alterations in the depth of the secondary eclipse. In the vast majority of DPVs, we directly observe the accretion disk during this orbital phase. In some cases, it has already been determined that the changes observed in the orbital light curves are due to structural variations in the accretion disk, stemming from variable mass transfer rate (e.g., Mennickent & Djurašević 2021). The hypothesis linking changes in mass transfer rate to a magnetic dynamo acting on the secondary component of DPVs requires observational evidence. Focusing on DPVs displaying notable changes in their light curves during the long cycle is essential. Validating this hypothesis demands spectroscopic observations not only to determine the system's fundamental parameters but also to conclusively provide evidence of structural changes in the accretion disk through spectroscopy (e.g., Armeni & Shore 2022).

Moreover, understanding the evolutionary state of the donor star holds particular interest due to its potential role in the DPV phenomenon. Generating evolutionary models via MESA for those systems where precise fundamental parameters have been determined will be crucial to comprehend and compare the evolution of both components in various DPV systems.

## 5. CONCLUSION

We analyzed 398 systems showing a variable O'Connell effect. Of these, 41% show cyclic changes of the O'Connell effect, with variation periods ranging from 17 to 360 days. In these binaries, we note that the estimated rotation periods for spotted stars is up to 3% longer than the orbital period. On the other hand, 59% of systems analyzed show non-cyclic changes of the O'Connell effect, and a large part of the spotted stars have rotational periods very close to the orbital periods.

For the 98 DPVs studied, we note that 70% show changes in the depths of the secondary minimum throughout the long cycle. Some 60% show a behavior similar to that of OGLE-LMC-DPV-097, i.e., a deeper secondary minimum at the maximum of the long cycle. Meanwhile, 10% show the opposite, with OGLE-BLG-ECL-157529 being an extreme example for this group. The rest of the DPVs do not show considerable changes and 87% of the binaries in this group have been categorized as ELL DPVs. Finally, we have analyzed the evolutionary status of OGLE-BLG-ECL-157529. It is in the case-B mass transfer phase and the system had initial masses of 3.2-2.9  $M_{\odot}$  for the secondary and primary component, respectively, with an initial orbital period of 6 days.

## Acknowledgements

JG acknowledges ANID project 21202285. JG and REM acknowledges support by BASAL Centro de Astrofísica y Tecnologías Afines (CATA) project FB210003. REM acknowledges FONDECYT 1190621. During work on this paper, J. Petrović was financially supported by the Ministry of Science, Technological Development and Innovation of the Republic of Serbia through contract no. 451-03-66/2024-03/200002.

## References

- Applegate, J. H.: 1992, *ApJ*, **385**, 621.  
 Armeni, A. & Shore S. N.: 2022, *A&A*, **664**, A103.  
 Balaji, B., et al.: 2015, *MNRAS*, **448**, 429.

- Cui, K., et al.: 2020, *ApJ*, **898**, 136.
- Garcés L., J., et al.: 2018, *MNRAS: Letters*, **477**, L11-L15.
- Giles, H. A. C., et al.: 2017, *MNRAS*, **472**, 1618.
- Matijevič, G., et al.: 2012, *AJ*, **143**, 123.
- Mennickent, R. E., et al.: 2003, *A&A*, **399**, L47.
- Mennickent, R. E., et al.: 2012, *MNRAS*, **427**, 607.
- Mennickent, R. E., et al.: 2015, *MNRAS*, **448**, 1137.
- Mennickent, R. E., et al.: 2017, *Serb. Astron. J.*, **194**, 1-27.
- Mennickent, R. E., et al.: 2018, *PASP*, **130**, 094203.
- Mennickent, R. E., et al.: 2020, *A&A*, **641**, 8.
- Mennickent, R. E. & Djurašević, G.: 2021, *A&A*, **653**, A89.
- Niu, Hu-Biao, et al.: 2022, *Research in Astronomy and Astrophysics*, **1**, 015016.
- O'Connell, D.: 1951, *Publication of the Riverview College Observatory*, **2**, 85.
- Paxton, B., et al.: 2011, *ApJS*, **192**, 3.
- Paxton, B., et al.: 2013, *ApJS*, **208**, 4.
- Paxton, B., et al.: 2015, *ApJS*, **220**, 15.
- Pi, Q., et al.: 2019, *ApJ*, **877**, 75.
- Poleski, R., et al.: 2010, *Acta Astron.*, **60**, 179.
- Richards, M. & Albright, G.: 1993, *Astrophysical Journal Supplement*, **88**, 199.
- Rojas García, G., et al.: 2021, *The Astrophysical Journal*, **922**, 30.
- Savitzky, A., & Golay, M. J. E.: 1964, *Analytical Chemistry*, **36**, 1627
- Schleicher, D. R. G. & Mennickent, R. E., *A&A*, **602**, 10.
- Shi, X., et al.: 2021, *The Astronomical Journal*, **161**, 46.
- Tran, K., et al.: 2013, *ApJ*, **774**, 14.
- Xiang, Yue, et al.: 2020, *MNRAS*, **492**, 3647-3656.
- Zahn J. P.: 1975, *A&A*, **41**, 329.
- Zahn J. P.: 1977, *A&A*, **57**, 383.
- Zechmeister, M. & Kurster, M.: 2008, *A&A*, **496**, 577.